 Proceedings of ICCES'08, pp.117-133

A Meshless Local Petrov-Galerkin Method for the Analysis of Cracks in the Isotropic Functionally Graded Material

K. Y. Liu[1,2], S. Y. Long[1,2,3] and G. Y. Li[1]

Summary

A meshless local Petrov-Galerkin method (MLPG)[1] for the analysis of cracks in isotropic functionally graded materials is presented. The meshless method uses the moving least squares (MLS) to approximate the field unknowns. The shape function has not the Kronecker Delta properties for the trial-function-interpolation, and a direct interpolation method is adopted to impose essential boundary conditions. The MLPG method does not involve any domain and singular integrals to generate the global effective stiffness matrix if body force is ignored; it only involves a regular boundary integral. The material properties are smooth functions of spatial coordinates and two interaction integrals[2,3] are used for the fracture analysis. Two numerical examples including both mode-I and mixed-mode problems are presented to calculated the stress intensity factors (SIFs) by the proposed method. Example problems in functionally graded materials are presented and compared with available reference solutions. A good agreement obtained show that the proposed method possesses no numerical difficulties.

keywords: MLPG; functionally graded material; interaction integral; Stress intensity factor

Introduction

The functionally graded material (FGM) has been applied in the development of structure components in the aeronautic and astronautic domains, which possesses gradually and continuously varying composition and structure, and its corresponding properties vary gradually along thickness. This material gradient can relax the stress concentration, weak the residual stress and improve the resistive ability of heat impact. Due to the reasons of technology, working conditions and some other factors, lots of cracks easily appear in a structure with FGM. The crack initiation and growth is the dominant type of failure in FGM. Hence, It's very important to design the components of FGM and improve the fracture toughness. Since material parameters of FGM are the function of spatial coordinates, this makes it difficult to obtain the analytic solutions for complex problems. Many engineering problems should be solved by numerical methods.

At present, the finite element method (FEM) is used generally for analysis of FGM [4−7]. FEM has a big limitation continuously remeshing the finite element

[1]State Key Laboratory of Advanced Design and Manufacture for Vehicle Body
[2]College of Mechanics and Aerospace Engineering , Hunan University, Changsha 410082, China
[3]Corresponding author. Tel.: +86-0731-8822114. E-mail address: sylong@hnu.cn

model involving a crack propagation. In recent years, various meshless methods have been developed to solve fracture mechanics problems[8−10]. The Meshless methods use a set of nodes scattered within the problem domain and on boundaries of domain. These nodes do not form a mesh meaning it does not need any information on the relationship between nodes for the interpolation of the unknown field variables. Since no element connectivity data is required, the remeshing characteristic of FEM is avoided. So, the meshless methods show a great potential to solve problems involving cracks.

The MLPG method, presented by Atluri and Zhu[1], is a very promising method for solving partial differential equations. Remarkable successes of the MLPG method have been reported in solving the potential problem, the convection-diffusion problem and the non-linear boundary problem by Atluri et al[1,11,12]; the fracture mechanics problem by Kim and Atluri[13]. In this paper, the MLPG method is used to analyze cracks in Isotropic functionally graded materials.

Crack-tip fields in FGM[14]

Consider a plane elasticity problem with a finite crack of length $2a$ lying in a medium with modulus of elasticity $E^*(x,y)$ and Poisson's ratio $\nu^*(x,y)$ varying with spatial coordinates, as shown in Fig.1 The governing equation of the Airy's stress function ϕ is

$$\nabla^2\left(\frac{1}{E^*}\nabla^2\phi\right)-\frac{\partial^2}{\partial y^2}\left(\frac{1+\nu^*}{E^*}\right)\frac{\partial^2\phi}{\partial x^2}-\frac{\partial^2}{\partial x^2}\left(\frac{1+\nu^*}{E^*}\right)\frac{\partial^2\phi}{\partial y^2} +2\frac{\partial^2}{\partial x\partial y}\left(\frac{1+\nu^*}{E^*}\right)\frac{\partial^2\phi}{\partial x\partial y}=0 \quad (1)$$

where $E^*(x,y)$, $\nu^*(x,y)$are given by $E(x,y)$ and $\nu(x,y)$ under a plane stress condition and by $E(x,y)/\left[1-\nu(x,y)^2\right]$, $E(x,y)/\left[1-\nu(x,y)\right]$ under a plane strain condition, and ∇^2 is a Laplacian operator. Upon expanding the above equation, the first term in the governing equation involves the bi-harmonic term identical to the homogeneous material, and the remaining terms involve the spatial derivatives of the material properties[2]. The elastic stress and displacement fields in FGM can be derived using the stress function in variable separable form, the same as the homogenous case. Hence, the singular stress field near the crack tip can be given

as

$$\sigma_{11}(r,\theta) = \frac{K_{\mathrm{I}}}{\sqrt{2\pi r}} f_{11}^{\mathrm{I}}(\theta) + \frac{K_{\mathrm{II}}}{\sqrt{2\pi r}} f_{11}^{\mathrm{II}}(\theta) \tag{2}$$

$$\sigma_{12}(r,\theta) = \frac{K_{\mathrm{I}}}{\sqrt{2\pi r}} f_{12}^{\mathrm{I}}(\theta) + \frac{K_{\mathrm{II}}}{\sqrt{2\pi r}} f_{12}^{\mathrm{II}}(\theta) \tag{3}$$

$$\sigma_{22}(r,\theta) = \frac{K_{\mathrm{I}}}{\sqrt{2\pi r}} f_{22}^{\mathrm{I}}(\theta) + \frac{K_{\mathrm{II}}}{\sqrt{2\pi r}} f_{22}^{\mathrm{II}}(\theta) \tag{4}$$

where$r$ and θ are polar coordinates with the crack tip as an origin, K_{I} and K_{II} are the SIF of mode-I and mode-II, respectively, and $f_{ij}^{\mathrm{I}}(\theta)$, $f_{ij}^{\mathrm{II}}(\theta)(i,j=1,2)$ are the standard angular functions identical to homogeneous case.

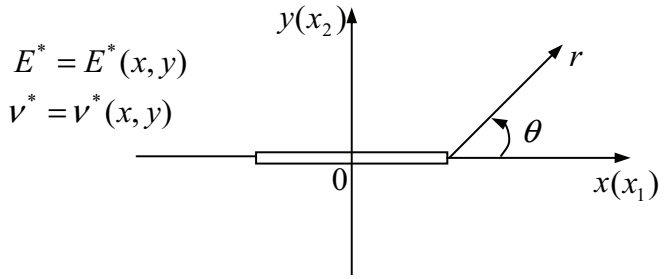

Figure 1: Crack geometry in FGM

The strain singular fields near the crack tip can be obtained by Eq.(2)∼Eq.(4)

$$\varepsilon_{ij} = S_{ijkl}(0)\sigma_{kl} \tag{5}$$

where $S_{ijkl}(0)$ is a component of flexibility tensor near the crack tip. Similarly, the displacement field can be written as

$$u_1(r,\theta) = \frac{1}{G_{tip}}\sqrt{\frac{r}{2\pi}}\left[K_{\mathrm{I}} g_1^{\mathrm{I}}(\theta) + K_{\mathrm{II}} g_1^{\mathrm{II}}(\theta)\right] \tag{6}$$

$$u_2(r,\theta) = \frac{1}{G_{tip}}\sqrt{\frac{r}{2\pi}}\left[K_{\mathrm{I}} g_2^{\mathrm{I}}(\theta) + K_{\mathrm{II}} g_2^{\mathrm{II}}(\theta)\right] \tag{7}$$

where $G_{tip} = E_{tip}/[2(1+\nu_{tip})]$ is shear modulus, E_{tip}, ν_{tip} are elastic modulus and Poisson's ratio, respectively, all calculated at the crack tip, and the $g_{ij}^{\mathrm{I}}(\theta)$, $g_{ij}^{\mathrm{II}}(\theta)$ $(i,j=1,2)$ are the standard angular functions identical to homogeneous case. Even though the material gradient does not influence the stress field distribution near the tip, but it influences distinctly the magnitude of SIFs.

The energy release rate for a crack in FGM is given by

$$G = \frac{K_{\mathrm{I}}^2}{E_{tip}} + \frac{K_{\mathrm{II}}^2}{E_{tip}} \tag{8}$$

It should be noted that the material gradient affects size of the region in which homogeneous solution is valid, and so the stress field distribution is different at the location far from the crack tip for homogeneous and non-homogeneous materials.

J-integral and M-integral in FGM[15]

A key of the research of fracture problems is how to computer J-integral. In homogeneous materials, J-integral is path independent. However, in FGM it is path dependent.

J-integral in homogeneous materials can be written as

$$J = \int_{\Gamma} \left(W\delta_{1j} - \sigma_{ij}\frac{\partial u_i}{\partial x_1} \right) n_j \mathrm{d}\Gamma \tag{9}$$

where$W = \sigma_{ij}\varepsilon_{ij}/2 = \varepsilon_{ij}D_{ijkl}\varepsilon_{kl}/2$ is a strain energy density for the linear elastic material model, n_j is an unit outward normal to a contour Γ around the crack tip, and D_{ijkl} is a constitutive tensor. Using the divergence theorem, Eq.(9) can be converted into an equivalent domain form written as

$$J = \int_A \left(\sigma_{ij}\frac{\partial u_i}{\partial x_1} - W\delta_{1j} \right) \frac{\partial q}{\partial x_j} \mathrm{d}A + \int_A \frac{\partial}{\partial x_j} \left(\sigma_{ij}\frac{\partial u_i}{\partial x_1} - W\delta_{1j} \right) q \mathrm{d}A \tag{10}$$

where A is area inside the contour and q is an arbitrary differentiable function. Expanding the above equation is given as

$$\begin{aligned} J = &\int_A \left(\sigma_{ij}\frac{\partial u_i}{\partial x_1} - W\delta_{1j} \right) \frac{\partial q}{\partial x_j} \mathrm{d}A \\ &+ \int_A \left(\frac{\partial \sigma_{ij}}{\partial x_j}\frac{\partial u_i}{\partial x_1} + \sigma_{ij}\frac{\partial^2 u_i}{\partial x_j \partial x_1} - \sigma_{ij}\frac{\partial \varepsilon_{ij}}{\partial x_1} - \frac{1}{2}\varepsilon_{ij}\frac{\partial D_{ijkl}}{\partial x_1}\varepsilon_{kl} \right) q \mathrm{d}A \end{aligned} \tag{11}$$

Considering equilibrium equation ($\partial\sigma_{ij}/\partial x_j = 0$), compatibility conditions ($\frac{\partial u_i}{\partial x_j} = \frac{1}{2}\left(\frac{\partial u_i}{\partial x_j} + \frac{\partial u_j}{\partial x_i}\right)$) and $\frac{\partial D_{ijkl}}{\partial x_1} = 0$ in homogenous materials, the second integrand of Eq. (11) vanishes, and it reduce to

$$J = \int_A \left(\sigma_{ij}\frac{\partial u_i}{\partial x_1} - W\delta_{1j} \right) \frac{\partial q}{\partial x_j} \mathrm{d}A \tag{12}$$

Consider two independent equilibrium states of a cracked body. Assume state 1 to be an actual state with specified boundary conditions, and state 2 to be an auxiliary state. Superposition of J-integrals of two states leads to another J-integral for state S

$$J^{(S)} = \int_A \left(\left[(\sigma_{ij}^{(1)} + \sigma_{ij}^{(2)}) \right] \frac{\partial (u_i^{(1)} + u_i^{(2)})}{\partial x_1} - W^{(S)}\delta_{1j} \right) \frac{\partial q}{\partial x_j} \mathrm{d}A \tag{13}$$

where $W^{(S)} = \frac{1}{2}(\sigma_{ij}^{(1)} + \sigma_{ij}^{(2)})(\varepsilon_{ij}^{(1)} + \varepsilon_{ij}^{(2)})$.

For FGM, equilibrium equation and compatibility conditions are still satisfied, the material gradient term is not constant any more and is a function of spatial coordinates. The second integrand of Eq. (11) does not entirely vanish. So Eq. (11) can be rewritten as

$$\tilde{J} = \int_A \left(\sigma_{ij} \frac{\partial u_i}{\partial x_1} - W \delta_{1j} \right) \frac{\partial q}{\partial x_j} \mathrm{d}A + \int_A \frac{1}{2} \varepsilon_{ij} \frac{\partial D_{ijkl}}{\partial x_1} \varepsilon_{kl} q \mathrm{d}A \tag{14}$$

By comparing Eq. (14) to Eq. (12), J-integral for FGM is in addition of the second domain integral in Eq. (14). The integrands in the second domain integral have singularity of order r^{-1} when an integral path is very close to the crack tip, but the total integral term has order r^1. In this case, the second integral can be negligible. The evaluation of $\tilde{J}$-integral is almost the same as that of homogeneous materials. $\tilde{J}$-integral must be accurately calculated for a relative large integral domain.

When the direction of a crack is not parallel to the direction of the material gradient, even under symmetric loads, stress and displacement fields at the crack tip are mixed-mode due to un-symmetry of FGM. For this situation, M-integral is generally adopted to calculate SIFs. $\tilde{J}$-integral Eq. (13) for the state S can be rewritten as

$$\begin{aligned} \tilde{J}^{(S)} = \int_A & \left(\left(\sigma_{ij}^{(1)} + \sigma_{ij}^{(2)} \right) \frac{\partial \left(u_i^{(1)} + u_i^{(2)} \right)}{\partial x_1} - W^{(S)} \delta_{1j} \right) \frac{\partial q}{\partial x_j} \mathrm{d}A \\ & + \int_A \frac{\partial}{\partial x_j} \left(\left(\sigma_{ij}^{(1)} + \sigma_{ij}^{(2)} \right) \frac{\partial \left(u_i^{(1)} + u_i^{(2)} \right)}{\partial x_1} - W^{(S)} \delta_{1j} \right) q \mathrm{d}A \end{aligned} \tag{15}$$

According Eq. (15), the evaluation of $\tilde{J}$-integral depends on how the auxiliary field is selected. In this study, the homogeneous and the non-homogeneous auxiliary fields are adopted to calculate $\tilde{J}$-integral.

Firstly, consider a homogeneous auxiliary field, and select Eqs. (2)–(4) and Eqs. (6)–(7) as the auxiliary stress and displacement fields, respectively. Thus $D_{ijkl}$is a constant constitutive tensor evaluated at the crack tip. Hence, both equilibrium equation and compatibility condition are satisfied in the homogeneous aux-

iliary field. Then, Eq.(15) can be written as

$$\tilde{J}^{(S)} = \int_A \left(\left(\sigma_{ij}^{(1)} + \sigma_{ij}^{(2)} \right) \frac{\partial \left(u_i^{(1)} + u_i^{(2)} \right)}{\partial x_1} - \left(W^{(1)} + W^{(2)} + W^{(1,2)} \right) \delta_{1j} \right) \frac{\partial q}{\partial x_j} \mathrm{d}A$$
$$+ \int_A \frac{1}{2} \left(-\varepsilon_{ij}^{(1)} \frac{\partial D_{ijkl}}{\partial x_1} \varepsilon_{kl}^{(1)} + \sigma_{ij}^{(1)} \frac{\partial \varepsilon_{ij}^{(2)}}{\partial x_1} - \frac{\partial \sigma_{ij}^{(2)}}{\partial x_1} \varepsilon_{ij}^{(1)} + \sigma_{ij}^{(2)} \frac{\partial \varepsilon_{ij}^{(1)}}{\partial x_1} - \frac{\partial \sigma_{ij}^{(1)}}{\partial x_1} \varepsilon_{ij}^{(2)} \right) q \mathrm{d}A \tag{16}$$

Eq. (16) can be rewritten as

$$\tilde{J}^{(S)} = \tilde{J}^{(1)} + \tilde{J}^{(2)} + \tilde{M}^{(1,2)}, \tag{17}$$

where

$$\tilde{J}^{(1)} = \int_A \left(\sigma_{ij}^{(1)} \frac{\partial u_i^{(1)}}{\partial x_1} - W^{(1)} \delta_{1j} \right) \frac{\partial q}{\partial x_j} \mathrm{d}A + \int_A \frac{1}{2} \varepsilon_{ij}^{(1)} \frac{\partial D_{ijkl}}{\partial x_1} \varepsilon_{kl}^{(2)} q \mathrm{d}A, \tag{18}$$

$$\tilde{J}^{(2)} = \int_A \left(\sigma_{ij}^{(2)} \frac{\partial u_i^{(2)}}{\partial x_1} - W^{(2)} \delta_{1j} \right) \frac{\partial q}{\partial x_j} \mathrm{d}A \tag{19}$$

are $\tilde{J}$-integral for state 1 and state 2, respectively, and

$$\tilde{M}^{(1,2)} = \int_A \left(\sigma_{ij}^{(1)} \frac{\partial u_i^{(2)}}{\partial x_1} + \sigma_{ij}^{(2)} \frac{\partial u_i^{(1)}}{\partial x_1} - W^{(1,2)} \delta_{1j} \right) \frac{\partial q}{\partial x_j} \mathrm{d}A$$
$$+ \int_A \frac{1}{2} \left(\sigma_{ij}^{(1)} \frac{\partial \varepsilon_{ij}^{(2)}}{\partial x_1} - \frac{\partial \sigma_{ij}^{(2)}}{\partial x_1} \varepsilon_{ij}^{(1)} + \sigma_{ij}^{(2)} \frac{\partial \varepsilon_{ij}^{(1)}}{\partial x_1} - \frac{\partial \sigma_{ij}^{(1)}}{\partial x_1} \varepsilon_{ij}^{(2)} \right) q \mathrm{d}A \tag{20}$$

is the interaction integral defined for FGM.

Secondly, consider a non-homogeneous auxiliary field, and still select Eqs. (2)–(4) and Eqs. (6)–(7) as the auxiliary stress and displacement fields, respectively. Thus D_{ijkl} is not a constant tensor and varies with the spatial coordinates. The auxiliary stress field satisfies the equilibrium equation and the auxiliary strain field is not compatible with the auxiliary displacement field ($\partial u_i / \partial x_j \neq \frac{1}{2}(\partial u_j \partial x_i$

$+\partial u_i/\partial x_j)$). Then, Eq.(15) can be rewritten as

$$\tilde{J}^{(S)} = \int_A \left(\left(\sigma_{ij}^{(1)} + \sigma_{ij}^{(2)} \right) \frac{\partial \left(u_i^{(1)} + u_i^{(2)} \right)}{\partial x_1} - \left(W^{(1)} + W^{(2)} + W^{(1,2)} \right) \delta_{1j} \right) \frac{\partial q}{\partial x_j} \mathrm{d}A$$
$$+ \int_A \left[\left(\sigma_{ij}^{(1)} + \sigma_{ij}^{(2)} \right) \left(\frac{\partial^2 u_i^{(2)}}{\partial x_j \partial x_1} - \frac{\partial \varepsilon_{ij}^{(2)}}{\partial x_1} \right) - \frac{1}{2} \left(\varepsilon_{ij}^{(1)} + \varepsilon_{ij}^{(2)} \right) \frac{\partial D_{ijkl}}{\partial x_1} \left(\varepsilon_{kl}^{(1)} + \varepsilon_{kl}^{(2)} \right) \right] q \mathrm{d}A \tag{21}$$

where

$$\tilde{J}^{(1)} = \int_A \left(\sigma_{ij}^{(1)} \frac{\partial u_i^{(1)}}{\partial x_1} - W^{(1)} \delta_{1j} \right) \frac{\partial q}{\partial x_j} \mathrm{d}A + \int_A \frac{1}{2} \varepsilon_{ij}^{(1)} \frac{\partial D_{ijkl}}{\partial x_1} \varepsilon_{kl}^{(1)} q \mathrm{d}A \tag{22}$$

$$\tilde{J}^{(2)} = \int_A \left(\sigma_{ij}^{(2)} \frac{\partial u_i^{(2)}}{\partial x_1} - W^{(2)} \delta_{1j} \right) \frac{\partial q}{\partial x_j} \mathrm{d}A$$
$$+ \int_A \left[\sigma_{ij}^{(2)} \left(\frac{\partial^2 u_i^{(2)}}{\partial x_j \partial x_1} - \frac{\partial \varepsilon_{ij}^{(2)}}{\partial x_1} \right) - \frac{1}{2} \varepsilon_{ij}^{(1)} \frac{\partial D_{ijkl}}{\partial x_1} \varepsilon_{kl}^{(2)} \right] q \mathrm{d}A \tag{23}$$

are $\tilde{J}$-integral for state 1 and state 2, respectively, and

$$\tilde{M}^{(1,2)} = \int_A \left(\sigma_{ij}^{(1)} \frac{\partial u_i^{(2)}}{\partial x_1} + \sigma_{ij}^{(2)} \frac{\partial u_i^{(1)}}{\partial x_1} - W^{(1,2)} \delta_{1j} \right) \frac{\partial q}{\partial x_j} \mathrm{d}A$$
$$+ \int_A \left[\sigma_{ij}^{(1)} \left(\frac{\partial^2 u_i^{(2)}}{\partial x_j \partial x_1} - \frac{\partial \varepsilon_{ij}^{(2)}}{\partial x_1} \right) - \varepsilon_{ij}^{(1)} \frac{\partial D_{ijkl}}{\partial x_1} \varepsilon_{kl}^{(2)} \right] q \mathrm{d}A \tag{24}$$

is the interaction integral for FGM.

Stress intensity factor

For linear elastic solids, J-integral represents an energy release rate, and similarly, $\tilde{J}$-integral for FGM can be represented as

$$\tilde{J} = \frac{1}{E_{tip}} (K_{\mathrm{I}}^2 + K_{\mathrm{II}}^2) \tag{25}$$

Regardless of what the auxiliary field are selected, Applying Eq. (25) to state

1,2,and S yields

$$\tilde{J}^{(1)} = \frac{1}{E_{tip}}\left[\left(K_{\mathrm{I}}^{(1)}\right)^2 + \left(K_{\mathrm{II}}^{(1)}\right)^2\right] \tag{26}$$

$$\tilde{J}^{(2)} = \frac{1}{E_{tip}}\left[\left(K_{\mathrm{I}}^{(2)}\right)^2 + \left(K_{\mathrm{II}}^{(2)}\right)^2\right] \tag{27}$$

$$\tilde{J}^{(S)} = \tilde{J}^{(1)} + \tilde{J}^{(2)} + \frac{2}{E_{tip}}(K_{\mathrm{I}}^{(1)}K_{\mathrm{I}}^{(2)} + K_{\mathrm{II}}^{(1)}K_{\mathrm{II}}^{(2)}) \tag{28}$$

Comparing Eq. (17) to Eq. (28), we have

$$\tilde{M}^{(1,2)} = \frac{2}{E_{tip}}(K_{\mathrm{I}}^{(1)}K_{\mathrm{I}}^{(2)} + K_{\mathrm{II}}^{(1)}K_{\mathrm{II}}^{(2)}) \tag{29}$$

Selecting state 1 as an actual state of the considered problem, and using asymptotic solutions of mode I or II as the auxiliary state 2, SIFs for FGM can be derived as

$$K_{\mathrm{I}}^{(1)} = \frac{\tilde{M}^{(1,\mathrm{I})}E_{tip}^*}{2} \tag{30}$$

or

$$K_{\mathrm{II}}^{(1)} = \frac{\tilde{M}^{(1,\mathrm{II})}E_{tip}^*}{2} \tag{31}$$

where $\tilde{M}^{(1,\mathrm{I})}$ and $\tilde{M}^{(1,\mathrm{II})}$ are two interaction integrals for mode I and II, respectively, and can be calculated using either Eq. (20) or Eq. (24).

The moving least square approximation and meshless shape function

Consider an unknown function of a field variable $u(\mathbf{x})$ in a domain,Ω_x. The moving least squares approximation of $u(\mathbf{x})$ is defined at $\mathbf{x}$ as

$$u^h(\mathbf{x}) = \mathbf{p}^T(\mathbf{x})\mathbf{a}(\mathbf{x}), \forall \mathbf{x} \in \Omega_x \tag{32}$$

where $\mathbf{p}^T(\mathbf{x})$ is a complete monomial basis function of order m and $\mathbf{a}(\mathbf{x})$ is a vector containing coefficients $a_j(\mathbf{x})$, $j = 1,2,\cdots,m$, which are functions of the space coordinates $\mathbf{x} = [x,y,z]^T$. For the two-dimensional problem, a complete monomial basis function is chosen as linear basis function:

$$\mathbf{p}^T(\mathbf{x}) = \begin{bmatrix}1 & x & y\end{bmatrix}, \quad m = 3 \tag{33}$$

quadratic basis function:

$$\mathbf{p}^T(\mathbf{x}) = \begin{bmatrix}1 & x & y & x^2 & xy & y^2\end{bmatrix}, \quad m = 6 \tag{34}$$

When solving problems involving cracks, $\sqrt{r}$, the triangular function and its combinations in linear elastic fracture mechanics[9] are included in the basis, i.e.

$$\mathbf{p}^T(\mathbf{x}) = \begin{bmatrix} 1 & x & y & \sqrt{r}\cos\frac{\theta}{2} & \sqrt{r}\sin\frac{\theta}{2} & \sqrt{r}\sin\frac{\theta}{2}\sin\theta & \sqrt{r}\cos\frac{\theta}{2}\sin\theta \end{bmatrix} \quad (35)$$

The coefficient vector $\mathbf{a}(\mathbf{x})$ in Eq. (32) can be obtained by minimizing a weighted, discrete L_2 norm as follows

$$J(\mathbf{x}) = \sum_{n=1}^{N} w(\mathbf{x}_n, \mathbf{x})[\mathbf{p}^T(\mathbf{x}_n)\mathbf{a}(\mathbf{x}) - \hat{u}_n]^2 \quad (36)$$

where N is the number of points in the neighborhood of $\mathbf{x}$ for which the weigh function $w(\mathbf{x}_n, \mathbf{x}) > 0$, and $\hat{u}_n$ is the fictitious nodal value of $\mathbf{u}$. This neighborhood of $\mathbf{x}$ is called the influence domain of$\mathbf{x}$, or influence circle in the two dimensional problem. In this study, a Gaussian weight function is chosen to approximate the function $u(\mathbf{x})$. The Gaussian weight function are written as

$$w(\mathbf{x}_n, \mathbf{x}) = \begin{cases} \frac{\exp\left[-(d_n/c_n)^{2k}\right] - \exp\left[-(r_n/c_n)^{2k}\right]}{1-\exp\left[-(r_n/c_n)^{2k}\right]}, & 0 \le d_n \le r_n \\ 0, & d_n \ge r_n \end{cases} \quad (37)$$

where $d_n = \|\mathbf{x} - \mathbf{x}_n\|$ is the distance from the sampling point $\mathbf{x}$ to a node $\mathbf{x}_n$, and r_n is a radius of the influence domain for the weight function $w(\mathbf{x}_n, \mathbf{x})$. Parameters c_n and k in Eq. (37) control the shape of the Gaussian weight function $w(\mathbf{x}_n, \mathbf{x})$. The parameter k can be taken as 1, and $c_n = r_n/4$.

The stationarity of J in Eq. (36) with respect to $\mathbf{a}(\mathbf{x})$ leads to the following linear relation between $\mathbf{a}(\mathbf{x})$ and $\hat{u}_n$

$$\mathbf{A}(\mathbf{x})\mathbf{a}(\mathbf{x}) = \mathbf{B}(\mathbf{x})\hat{\mathbf{u}} \quad (38)$$

where matrices $\mathbf{A}(\mathbf{x})$ and $\mathbf{B}(\mathbf{x})$ are defined by

$$\mathbf{A}(\mathbf{x}) = \mathbf{P}^T\mathbf{W}\mathbf{P} = \mathbf{B}(\mathbf{x})\mathbf{P} = \sum_{n=1}^{N} w(\mathbf{x}_n,\ \mathbf{x})\mathbf{p}(\mathbf{x}_n)\mathbf{p}^T(\mathbf{x}_n) \quad (39)$$

$$\mathbf{B}(\mathbf{x}) = \mathbf{P}^T\mathbf{W} = [w(\mathbf{x}_1, \mathbf{x})\mathbf{p}(\mathbf{x}_1), w(\mathbf{x}_2, \mathbf{x})\mathbf{p}(\mathbf{x}_2), \cdots, w(\mathbf{x}_N, \mathbf{x})\mathbf{p}(\mathbf{x}_N)] \quad (40)$$

$$\hat{\mathbf{u}}^T = [\hat{u}_1\ \hat{u}_2 \cdots \hat{u}_N] \quad (41)$$

Hence, we have

$$u^h(\mathbf{x}) = \sum_{n=1}^{N} \varphi_n(\mathbf{x})\hat{u}_n, \quad u^h(\mathbf{x}) \equiv u_n \neq \hat{u}_n, \mathbf{x} \in \Omega_x \quad (42)$$

where the shape function $\varphi_n(\mathbf{x})$ is defined by

$$\varphi_n(\mathbf{x}) = \sum_{m=1}^{M} p_m(\mathbf{x})[\mathbf{A}^{-1}(\mathbf{x})\mathbf{B}(\mathbf{x})]_{mn} \tag{43}$$

The partial derivatives of $\varphi_n(\mathbf{x})$ can be obtained as follows

$$\varphi_{n,k} = \sum_{m=1}^{M} [p_{m,k}(\mathbf{A}^{-1}\mathbf{B})_{mn} + p_m(\mathbf{A}^{-1}\mathbf{B}_{,k} + \mathbf{A}^{-1}_{,k}\mathbf{B})_{mn}] \tag{44}$$

where

$$\mathbf{A}^{-1}_{,k} = -\mathbf{A}^{-1}\mathbf{A}_{,k}\mathbf{A}^{-1} \tag{45}$$

The MLPG Formulation

Consider the following two-dimensional elasto-static problem on a domain Ω bounded by a boundary Γ

$$\sigma_{ij,j} + b_i = 0, \quad \text{in } \Omega \tag{46}$$

where σ_{ij} is a stress tensor, b_i is a body force. Boundary conditions are given as follows

$$u_i = \bar{u}_i, \quad on\Gamma_u, \tag{47a}$$

$$t_i = \sigma_{ij}n_j = \bar{t}_i, \quad on\Gamma_t \tag{47b}$$

where $\bar{u}_i$ and $\bar{t}_i$ are the prescribed displacement and traction on the boundary Γ_u and Γ_t, respectively. n_j is an unit outward normal to the boundary Γ. Γ_u and Γ_t are complementary subsets of Γ.

In MLPG method, the system equation is constructed node by node, which makes it possible to use different sets of equations for different nodes. In this study, we use two different sets of equations for the essential boundary nodes and not essential boundary nodes, respectively.

For a node $\mathbf{x}$ not located on the essential boundary, we start from a weak form over a local sub-domain Ω_s and use the MLS approximation to develop the present meshless local Petrov-Galerkin formulation in which the local sub-domain Ω_s is set to βd_i^1, β is a scaling factor for determining the sub-domain and d_i^1 is the distance to the nearest neighboring point from node i. Here we set $\beta \leq 1.0$ to make the sub-domain Ω_s not intersect with the essential boundary Γ_u, so a generalized local weak form of Eq. (46) over the local sub-domain Ω_s can be written as follows

$$\int_{\Omega_s} (\sigma_{ij,j} + b_i) v_i \mathrm{d}\Omega = 0 \tag{48}$$

where v_i is a test function. Using the following relationship

$$\sigma_{ij,j}v_i = (\sigma_{ij}v_i)_{,j} - \sigma_{ij}v_{i,j} \tag{49}$$

and the divergence theorem in Eq. (47) leads to

$$\int_{\Omega_s} (-\sigma_{ij}v_{i,j} + b_i v_i)\mathrm{d}\Omega + \int_{\partial\Omega_s} t_i v_i \mathrm{d}\Gamma = 0 \tag{50}$$

where $\partial\Omega_s$ is the boundary of sub-domain Ω_s, $t_i = \sigma_{ij}n_j$, and n_j is a unit outward normal to the boundary $\partial\Omega_s$. In general, $\partial\Omega_s = \Gamma_s \cup L_s$ with Γ_s being the part of the local boundary located on the global boundary and L_s being the other part of the local boundary over which no boundary condition is specified, i.e., $\Gamma_s = \partial\Omega_s \cap \Gamma$ and $\Gamma_s = \partial\Omega_s - L_s$.

It should be mentioned that Eq. (49) holds regardless of the size and the shape of Ω_s provided that Ω_s is smooth enough for the divergence theorem to apply. So, the shape of the sub-domain Ω_s can be taken to be a circle in the two-dimensional problem without loosing generality.

Applying the natural boundary condition, $t_i = \sigma_{ij}n_j = \bar{t}_i$ on Γ_{st} where $\Gamma_{st} = \partial\Omega_s \cap \Gamma_t$, we get

$$\int_{\Omega_s} \sigma_{ij}v_{i,j}\mathrm{d}\Omega - \int_{\Gamma_{su}} t_i v_i \mathrm{d}\Gamma = \int_{\Gamma_{st}} \bar{t}_i v_i \mathrm{d}\Gamma + \int_{\Omega_s} b_i v_i \mathrm{d}\Omega \tag{51}$$

In order to obtain the discretized system equations, the global problem domain Ω is represented by properly distributed field nodes. Using the MLS shape function to approximate the trial function for the displacement at a point $\mathbf{x}$

$$\mathbf{u}^h(\mathbf{x}) = \begin{Bmatrix} u \\ v \end{Bmatrix} = \begin{bmatrix} \varphi_1 & 0 & \cdots & \varphi_n & 0 \\ 0 & \varphi_1 & \cdots & 0 & \varphi_n \end{bmatrix} \begin{Bmatrix} u_1 \\ v_1 \\ \vdots \\ u_n \\ v_n \end{Bmatrix} = \mathbf{\Phi}\mathbf{u} \tag{52}$$

where n is the number of nodes in the support domain of a sampling point at $\mathbf{x}$, and $\mathbf{\Phi}$ is the matrix of the MLS shape functions.

Substitution of the MLS approximation Eq. (51) into Eq. (50) leads to the following nodal discretized system equation of MLPG for the Ith field node.

$$\int_{\Omega_s} \mathbf{G}^T(\mathbf{x},\mathbf{x}_I)\sigma\mathrm{d}\Omega - \int_{\Gamma_{su}} \mathbf{W}^T(\mathbf{x},\mathbf{x}_I)\mathbf{t}\mathrm{d}\Gamma = \int_{\Gamma_{st}} \mathbf{W}^T(\mathbf{x},\mathbf{x}_I)\bar{\mathbf{t}}\mathrm{d}\Gamma + \int_{\Omega_s} \mathbf{W}^T(\mathbf{x},\mathbf{x}_I)\mathbf{b}\mathrm{d}\Gamma \tag{53}$$

where

$$\sigma = \begin{Bmatrix} \sigma_{11} \\ \sigma_{22} \\ \sigma_{12} \end{Bmatrix}, \quad \mathbf{W}(\mathbf{x}, \mathbf{x}_I) = \begin{bmatrix} w_1(\mathbf{x}, \mathbf{x}_I) & 0 \\ 0 & w_2(\mathbf{x}, \mathbf{x}_I) \end{bmatrix} \quad \text{and} \quad \mathbf{G} = \begin{bmatrix} \frac{\partial w_1}{\partial x_1} & 0 \\ 0 & \frac{\partial w_2}{\partial x_2} \\ \frac{\partial w_1}{\partial x_2} & \frac{\partial w_2}{\partial x_1} \end{bmatrix} \tag{54}$$

Using constitutive and strain-displacement equations, we can have

$$\sigma = \mathbf{D}(\mathbf{x})\varepsilon = \sum_{j=1}^{n} \mathbf{D}\mathbf{B}_j \hat{\mathbf{u}}_j, \mathbf{t} = \begin{Bmatrix} t_1 \\ t_2 \end{Bmatrix} = \mathbf{n}\sigma = \sum_{j=1}^{n} \mathbf{n}\mathbf{D}\mathbf{B}_j \hat{\mathbf{u}}_j, \tag{55}$$

where B_j is the strain matrix about the jth node, $\mathbf{n}$ is a matrix of the unit outward normal to the boundary Γ_{st} and Γ_{su}, and $\mathbf{D}(\mathbf{x})$ is the material matrix for the plane stress problem. They are given by

$$\mathbf{B}_j = \begin{bmatrix} \frac{\partial \varphi_1}{\partial x_1} & 0 \\ 0 & \frac{\partial \varphi_2}{\partial x_2} \\ \frac{\partial \varphi_1}{\partial x_2} & \frac{\partial \varphi_2}{\partial x_1} \end{bmatrix}_j, \mathbf{n} = \begin{bmatrix} n_1 & 0 & n_2 \\ 0 & n_2 & n_1 \end{bmatrix}$$

and

$$\mathbf{D}(\mathbf{x}) = \frac{E(\mathbf{x})}{1-\nu^2(\mathbf{x})} \begin{bmatrix} 1 & \nu(\mathbf{x}) & 0 \\ \nu(\mathbf{x}) & 1 & 0 \\ 0 & 0 & \frac{1-\nu(\mathbf{x})}{2} \end{bmatrix} \tag{56}$$

Substitution of Eq. (54) into Eq. (52) leads to the following discretized systems of equations for the Ith field node.

$$\sum_{j=1}^{n} \mathbf{K}_I \hat{\mathbf{u}}_j = \mathbf{f}_I \tag{57}$$

where $\mathbf{K}_I$ is a matrix called the nodal stiffness matrix for the Ithfield node, which is computed using

$$\mathbf{K}_{Ij} = \int_{\Omega_s} \mathbf{G}^T \mathbf{D}\mathbf{B}_j \mathrm{d}\Gamma - \int_{\Gamma_{su}} \mathbf{W}^T \mathbf{N}\mathbf{D}\mathbf{B}_j \mathrm{d}\Gamma \tag{58}$$

$\mathbf{f}_I$ is a nodal force vector, which is computed using

$$\mathbf{f}_I = \int_{\Gamma_{st}} \mathbf{W}^T \bar{\mathbf{t}} \mathrm{d}\Gamma + \int_{\Omega_s} \mathbf{W}^T \mathbf{b} \mathrm{d}\Gamma \tag{59}$$

For the nodes located on the essential boundary, a direct interpolation method for the imposition of essential boundary conditions is introduced in this paper. This

method was proposed by G.R. Liu and L. Yan[15] to simplify the MLPG formulation. The direct interpolation method enforces the essential boundary conditions using the equation of the MLS approximation

$$u_I^h(\mathbf{x}) = \sum_{i=1}^{n} \phi_i(\mathbf{x}) u_i = \bar{u}_I \tag{60}$$

Eq. (59) is assembled directly into the system equations for field nodes to obtain the global system equation of

$$K\hat{U} = F \tag{61}$$

Note also that this direct approach of imposing essential boundary conditions destroys the symmetry of the stiffness matrix. Fortunately, this does not create additional problems, because the stiffness matrix created using MLPG is not symmetric originally.

Numerical examples

MLPG method with two interaction integrals is applied to calculate SIFs of cracks in FGM. In all examples, the elastic modulus is assumed to be spatially variable, and the Poisson's ratio is assumed to be constant. A fully enriched basis function is adopted in a part of domain around the crack tip, and a linear basis function is adopted in the rest of domain. For the numerical integration, 8×8 Gauss points are assigned in a sub-domain for the domain integral, and 9 Gauss points are assigned in a sub-boundary for the boundary integral.

Example 1: an edge-cracked plate under mode-I

An edge-cracked plate with length $L = 8$ unit, width $W = 1$ unit , and crack length a, subjected to the constant tensile stress loading, the linear stress loading and the constant strain loading, respectively, as shown in Fig.2, was discussed. The elastic modulus was assumed to be

$$E(x) = E_1 \exp(\eta x), \quad 0 \le x \le W \tag{62}$$

where $E_1 = E(0)$, $E_2 = E(W)$, and $\eta = \ln(\frac{E_2}{E_1})$. In computation, $E_1 = 1$ unit, $\frac{E_2}{E_1} = \exp(\eta) = 0.1,\ 0.2,\ 5,$ and 10, and $a = 0.2, 0.4, 0.5$ and 0.6 are used. The Poisson's ratio was held constant with $\nu = 0.3$. A plane strain condition was assumed.

Due to symmetry of geometry and load, one half of the plate was analyzed by the MLPG method shown in Fig. 3. Fig. 4 shows a meshless discretization consisting of 272 nodes. The shadow of domain with size $c \times b$, as shown in Fig.(3), was used to calculate M-integral.

Table 1-3 show the normalized mode-I SIFs $K_{\mathrm{I}}/\sigma_t\sqrt{\pi a}$, $K_{\mathrm{I}}/\sigma_b\sqrt{\pi a}$ and $K_{\mathrm{I}}/\sigma_0\sqrt{\pi a}$ for three types of loadings, respectively, where $\sigma_t = \sigma_b = 1$ unit, $\sigma_0 = E_1\varepsilon_0(1-\nu^2)$, $\varepsilon_0 = 1$ unit. The integral domain with size $c = 0.2$ and $b = 0.1$ unit

was used and the homogeneous auxiliary field is adopted for M-integral. The results show that SIFs obtained by the proposed method agree well with the solutions of references[2,17] for various combinations of E_2/E_1 and a/W. Table 4-6 show the results of the normalized mode-I SIFs with the different integral domain size under three types of loadings and two types of auxiliary fields. The results are accurate and independent of the size of the integral domain and the type of the auxiliary fields.

Example 2: a slanted edge-cracked plate under mixed mode

Consider a slanted edge-cracked plate with length $L = 2$ units, width $W = 1$ unit, and crack length $a = 0.4\sqrt{2}$ unit, inclination angle $\alpha = 45°$,as shown in Fig. 5. The elastic modulus was assumed to be

$$E(x) = E_1 \exp[\eta\,(x-0.5)], \quad 0 \le x \le W \tag{63}$$

where E_1 and η are two material parameters. In computation, $E_1 = 1$, $\eta = 0, 0.25$, 0.5, 0.75, and 1.0 ,and the Poisson's ratio $\nu = 0.3$ are used. A plane stress condition was assumed. The upper edge of the plate was subjected to the normal stress load $\sigma_{22}(x, L/2) = \bar{\varepsilon} E_1 \exp[\eta(x-0.5)]$, where $\bar{\varepsilon} = 1$ unit. The displacement constraint in y direction is applied to the bottom edge, i.e. $v\,(x, -L/2) = 0\,(0 \le x \le W)$. Besides, the displacement constraint in x direction is applied to a right node at the bottom edge, i.e. $u\,(W, -L/2) = 0$. Fig. 6 shows a meshless discretization consisting of 1004 nodes.

Table 7 shows the normalized SIFs $K_{\mathrm{I}}/\bar{\varepsilon}E_1\sqrt{\pi a}$ and $K_{\mathrm{II}}/\bar{\varepsilon}E_1\sqrt{\pi a}$ obtained by the proposed method with two types of auxiliary fields for several values of η and the integral domain size $b \times b = 0.1 \times 0.1$. The results obtained by the MLPG method agree well with that of Rao BN[2]. Table 8 shows the results of the normalized SIFs with the different integral domains and two types of auxiliary fields. The results are accurate and independent of the size of the integral domain and the type of the auxiliary fields.

Summary and conclusions

In this study, the MLPG method was used to calculate SIFs of cracks in FGM. In FGM, the elastic modulus is a function of spatial coordinates. Two interaction integral methods were applied to calculate M-integral. In two numerical examples, several material parameters and different integral domain sizes are considered to evaluate SIFs. The comparisons have been made between SIFs obtained by the proposed method and that by other methods. A good agreement obtained shows that the proposed method possesses no numerical difficulties in the analysis of cracks in FGM.

Acknowledgement

This work was supported by Natural Science Foundation of China

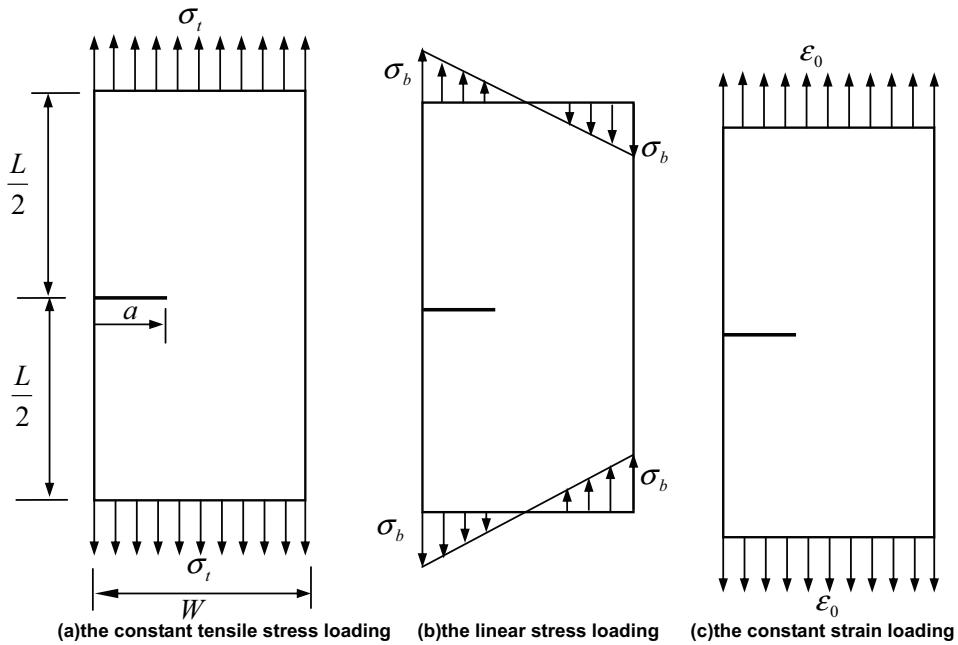

Figure 2: An edge-cracked plate under three types of mode-I loadings

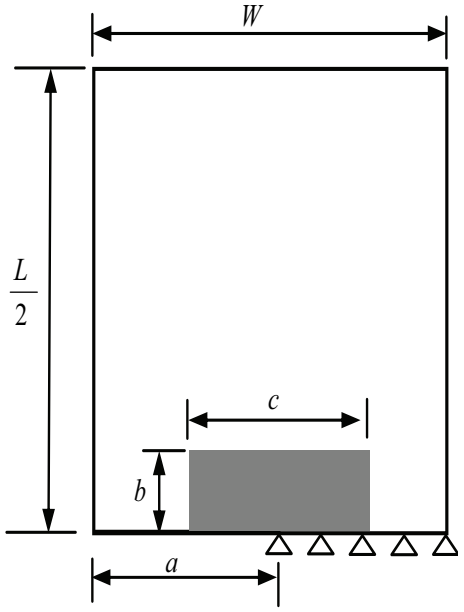

Figure 3: Half model and a domain for M-integral

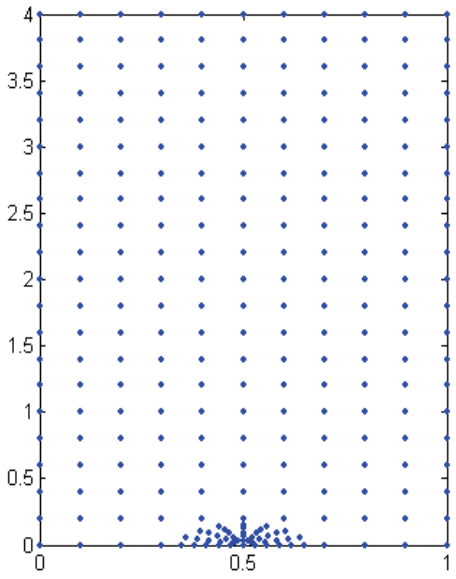

Figure 4: A meshless discretization (272 nodes)

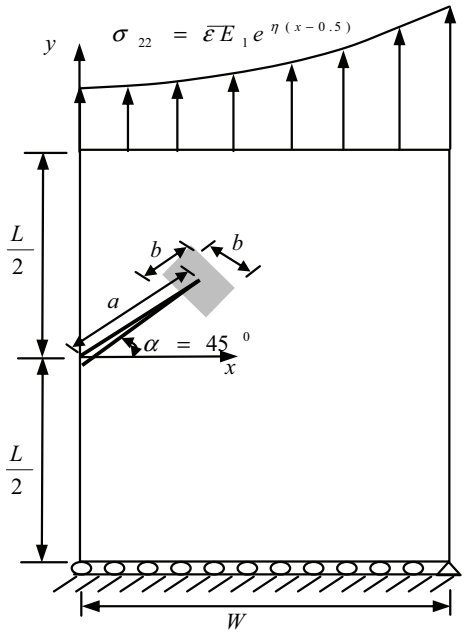

Figure 5: A slanted edge-cracked plate

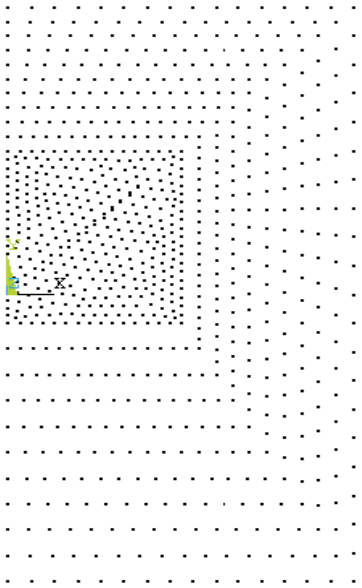

Figure 6: A meshless discretization (1004 nodes)

(No.10672055),The Key Project of NSFC of China (No.60635020) and The National Science Foundation for Outstanding Youth of China(No.50625519).

References

1. Atluri SN and Zhu T. A new meshless local Petrov-Galerkin (MLPG) approach in computational mechanics. Comput Mech, 1998, 22, 117-127.
2. Rao BN, Rahman S. Mesh-free analysis of cracks in isotropic functionally graded materials. Engineering Fracture Mechanics, 2003, 70, 1-27.
3. Rao BN, Rahman S. An interaction integral method for analysis of cracks in orthotropic functionally graded materials. Computational Mechanics, 2003, 23, 40-51.
4. Eischen JW. Fracture of nonhomogeneous materials. Int J Fract,1987, 34, 3-22.
5. Gu P, Asaro RJ. A simplified method for calculating the crack tip field of functionally graded materials using the domain integral. J Appl Mech, 1999, 66, 101-108.
6. Anlas G, Santare MH, Lambros J. Numerical calculation of stress intensity factors in functionally graded materials. Int J Fract, 2000, 104, 131-143.

7. Kim JH, Paulino GH. Finite element evaluation of mixed mode stress intensity factors in functionally graded materials. Int J Numer Meth Eng, 2002, 53(8), 1903-1935.
8. Rao BN, Rahman S. An efficient meshless method for fracture analysis of cracks. Comput Mech, 2000, 26, 398-408.
9. Belytschko T, Lu YY, Gu L. Crack propagation by element-free Galerkin methods. Eng Fract Mech, 1995, 51(2), 295-315.
10. Belytschko T, Tabbara M. Dynamic fracture using element-free Galerkin methods. Int J Numer Meth Eng, 1996, 39,923-938.
11. Lin H and Atluri S N. Meshless local Petrov-Galerkin (MLPG) method for convection-diffusion problems. Computer Modeling in Engineering & Sciences (CMES), 2000, 1, 45-60.
12. Atluri SN and Zhu T. A new meshless local Petrov-Galerkin (MLPG) approach to nonlinear problems in computer modeling and simulation. Computational Modeling and Simulation in Engineering, 1998, 3, 187-196.
13. Kim HG and Atluri SN. Arbitrary placement of secondary nodes, and error control, in the meshless local Petrov-Galerkin (MLPG) method. Computer Modeling in Engineering & Sciences (CMES), 2000, 1, 11-32.
14. Suresh S, Mortensen A. Fundamentals of functionally graded materials. London: IOM Communications Ltd.; 1998.
15. Rice JR. A path independent integral and the approximate analysis of strain concentration by notches and cracks. J Appl Mech, 1968, 35, 379-386.
16. Liu G.R., Yan L., A modified meshless local Petrov-Galerkin method for solid mechanics. In Advances in Computational Engineering and Sciences, Atluri N K and Brust F W, Eds., Tech. Science Press, Palmdale, CA, 2000, 1374-137.
17. Erdogan F., Wu B. H., The surface crack problem for a plate with functionally graded properties. J Appl Mech, 1997, 64, 449-56.

Table 1: The normalized mode-I SIF for an edge-cracked under the constant tensile stress loading

Method	$\frac{E_2}{E_1}$	$K_{\mathrm{I}}/\sigma_t\sqrt{\pi a}$			
		0.2	0.4	0.5	0.6
MLPG	0.1	1.3201	2.5809	3.5543	5.1205
	0.2	1.4023	2.4551	3.3209	4.7231
	5	1.1294	1.7502	2.3689	3.4610
	10	0.9976	1.5878	2.1797	3.2305
B.N.Rao et al.[2]	0.1	1.3374	2.5938	3.5472	4.9956
	0.2	1.4193	2.4657	3.3297	4.6905
	5	1.1269	1.7576	2.3772	3.4478
	10	0.9958	1.5890	2.1889	3.2167
Erdoganet al.[17]	0.1	1.2965	2.5699	3.5701	5.1890
	0.2	1.3956	2.4436	3.3266	4.7614
	5	1.1318	1.7483	2.3656	3.4454
	10	1.0019	1.5884	2.1762	3.2124

Table 2: The normalized mode-I SIF for an edge-cracked under the linear stress loading

Method	$\frac{E_2}{E_1}$	$K_{\mathrm{I}}/\sigma_b\sqrt{\pi a}$			
		0.2	0.4	0.5	0.6
MLPG	0.1	1.9102	1.9904	2.1734	2.5891
	0.2	1.6031	1.7413	1.9117	2.3837
	5	0.6798	0.9115	1.1728	1.5901
	10	0.5583	0.7986	1.0731	1.4410
B.N.Rao et al.[2]	0.1	1.9029	1.9539	2.1547	2.5484
	0.2	1.5976	1.7150	1.9322	2.3347
	5	0.6865	0.9319	1.1666	1.5626
	10	0.5635	0.8120	1.0447	1.4340
Erdoganet al.[17]	0.1	1.9040	1.9778	2.2151	2.1770
	0.2	1.5925	1.7210	1.9534	2.4037
	5	0.6871	0.9236	1.1518	1.5597
	10	0.5648	0.8043	1.0350	1.4286

Table 3: The normalized mode-I SIF for an edge-cracked under the constant strain loading

Method	$\frac{E_2}{E_1}$	$K_I/\sigma_0\sqrt{\pi a}$			
		0.2	0.4	0.5	0.6
MLPG	0.1	1.3112	1.8310	2.2917	3.0621
	0.2	1.3205	1.8903	2.3808	3.2332
	5	1.4904	2.5687	3.6781	5.5103
	10	1.5692	2.8410	4.3412	6.5112
B.N.Rao et al.[2]	0.1	1.3118	1.8241	2.2800	3.0100
	0.2	1.3186	1.8837	2.3966	3.2274
	5	1.4835	2.5819	3.6698	5.5708
	10	1.5557	2.8789	4.2234	6.6266
Erdoganet al.[17]	0.1	1.2963	1.8246	2.3140	3.1544
	0.2	1.3058	1.8751	2.4031	3.2981
	5	1.4946	2.5730	3.6573	5.5704
	10	1.5740	2.8736	4.2140	6.6319

Table 4: The normalized mode-I SIF for an edge-cracked under the constant tensile stress loading with two types of auxiliary fields and three different sizes of the integral domain

$b\times c$	$\frac{E_2}{E_1}$	$\frac{K_I}{\sigma_t\sqrt{\pi a}}(a=0.5)$	
		Homogeneous auxiliary field	Non-homogeneous auxiliary field
0.1×0.2	0.1	3.5543	3.5597
	0.2	3.3209	3.3271
	5	2.3689	2.3710
	10	2.1797	2.1823
0.1×0.3	0.1	3.5710	3.5735
	0.2	3.3352	3.3387
	5	2.3810	2.3841
	10	2.1903	2.1940
0.15×0.3	0.1	3.5823	3.5870
	0.2	3.3407	3.3462
	5	2.3894	2.3925
	10	2.1987	2.2003

Table 5: The normalized mode-I SIF for an edge-cracked under the linear stress loading with two types of auxiliary fields and three different sizes of the integral domain

$b \times c$	$\frac{E_2}{E_1}$	$\frac{K_I}{\sigma_b\sqrt{\pi a}}(a=0.5)$	
		Homogeneous auxiliary field	Non-homogeneous auxiliary field
0.1×0.2	0.1	2.1734	2.1785
	0.2	1.9117	1.9148
	5	1.1728	1.1750
	10	1.0731	1.0762
0.1×0.3	0.1	2.1841	2.1895
	0.2	1.9226	1.9265
	5	1.1819	1.1850
	10	1.0810	1.0832
0.15×0.3	0.1	2.1950	2.2003
	0.2	1.9318	1.9364
	5	1.1902	1.1946
	10	1.0887	1.0913

Table 6: The normalized mode-I SIF for an edge-cracked under the constant strain loading with two types of auxiliary fields and three different sizes of the integral domain

$b \times c$	$\frac{E_2}{E_1}$	$\frac{K_I}{\sigma_0\sqrt{\pi a}}(a=0.5)$	
		Homogeneous auxiliary field	Non-homogeneous auxiliary field
0.1×0.2	0.1	2.2917	2.2951
	0.2	2.3808	2.3858
	5	3.6781	3.6826
	10	4.3412	4.3490
0.1×0.3	0.1	2.3013	2.3052
	0.2	2.3891	2.3947
	5	3.6890	3.6981
	10	4.3572	4.3630
0.15×0.3	0.1	2.3095	2.3142
	0.2	2.3985	2.4035
	5	3.7012	3.7088
	10	4.3706	4.3721

Table 7: The normalized SIFs for a slanted edge-cracked plate with two types of auxiliary fields

Method	η	Homogeneous auxiliary field		Non-homogeneous auxiliary field	
		$K_{\mathrm{I}}/\bar{\varepsilon}E_1\sqrt{\pi a}$	$K_{\mathrm{II}}/\bar{\varepsilon}E_1\sqrt{\pi a}$	$K_{\mathrm{I}}/\bar{\varepsilon}E_1\sqrt{\pi a}$	$K_{\mathrm{II}}/\bar{\varepsilon}E_1\sqrt{\pi a}$
MLPG	0	1.462	0.621	1.462	0.621
	0.25	1.320	0.553	1.331	0.560
	0.5	1.209	0.498	1.215	0.502
	0.75	1.094	0.450	1.098	0.453
	1	0.995	0.407	0.998	0.409
B.N.Rao et al.[2]	0	1.448	0.610	1.448	0.610
	0.25	1.313	0.549	1.312	0.549
	0.5	1.193	0.495	1.190	0.495
	0.75	1.086	0.447	1.082	0.446
	1	0.990	0.405	0.986	0.404

Table 8: The normalized SIFs for a slanted edge-cracked plate with two types of auxiliary fields and three different sizes of the integral domain

$b \times b$	Homogeneous auxiliary field		Non-homogeneous auxiliary field	
	$K_{\mathrm{I}}/\bar{\varepsilon}E_1\sqrt{\pi a}$	$K_{\mathrm{II}}/\bar{\varepsilon}E_1\sqrt{\pi a}$	$K_{\mathrm{I}}/\bar{\varepsilon}E_1\sqrt{\pi a}$	$K_{\mathrm{II}}/\bar{\varepsilon}E_1\sqrt{\pi a}$
0.10×0.10	1.209	0.498	1.215	0.502
0.12×0.12	1.215	0.502	1.223	0.507
0.15×0.15	1.218	0.503	1.228	0.510
0.10×0.10	0.990	0.405	0.998	0.409
0.12×0.12	0.994	0.407	1.002	0.412
0.15×0.15	0.997	0.409	1.005	0.414